Exploration Geophysics

ISSN: 0812-3985 (Print) 1834-7533 (Online) Journal homepage: https://www.tandfonline.com/loi/texg20

Geophysical applications for Fe-rich emery exploration in the Elmacik area on the Menderes Massif (Turkey)

Ibrahim Aydin, Osman Uyanik, Erdinc Oksum & M. Selman Aydogan

To cite this article: Ibrahim Aydin, Osman Uyanik, Erdinc Oksum & M. Selman Aydogan (2011) Geophysical applications for Fe-rich emery exploration in the Elmacik area on the Menderes Massif (Turkey), Exploration Geophysics, 42:2, 159-166, DOI: 10.1071/EG09004

To link to this article: https://doi.org/10.1071/EG09004

CSIRO PUBLISHING
www.publish.csiro.au/journals/eg *Exploration Geophysics*, 2011, **42**, 159–166

Geophysical applications for Fe-rich emery exploration in the Elmacik area on the Menderes Massif (Turkey)

Ibrahim Aydin[1,4] Osman Uyanik[2,5] Erdinc Oksum[2] M. Selman Aydogan[3,4]

[1]Department of Geophysical Engineering, Engineering Faculty, Ankara University Besevler, 06100 Ankara, Turkey.
[2]Geophysics Department, Engineering Faculty, Suleyman Demirel University, 032260, Isparta, Turkey.
[3]Geology Department, Engineering Faculty, Balikesir University, 10145 Balikesir, Turkey.
[4]Formerly Suleyman Demirel University, Engineering Faculty, 032260 Isparta, Turkey.
[5]Corresponding author. Email: uyanik@mmf.sdu.edu.tr

Abstract. To determine the continuity of known Fe-rich emery horizons and to explore new deposits in the Elmacik area (Yatagan, Turkey), a geophysical survey was carried out using magnetic and electrical methods. Magnetic measurements were taken in the target area of 5 km^2 and a vertical electrical sounding technique was applied at 15 locations in the alluvial/eluvial (A/E) part of the area in order to explore possible placer emery horizons, and to investigate the thickness of the A/E assembly and any probable faults.

Significant magnetic anomalies occur in the vicinity of old and abandoned emery pits in the marbles of Mt Ismail. The anomalies in the marbles were caused by Fe-rich emery bodies, which did not crop out and were not more than 10 m deep. The magnetic anomalies in the A/E part of the area were weak in amplitude and may suggest small new placer emery deposits.

The result of the vertical electrical soundings indicated two fault zones, one in a N–S direction, and the other approximately in an E–W direction. The thickness of the A/E assembly varies from 2–3 m to 60–100 m. A low resistivity zone, which is located in the mid-east of the A/E part of the study area, correlates well with the long-wavelength magnetic anomaly. According to the survey results, further exploration activities should take place around abandoned emery pits.

Key words: electrical sounding, emery, magnetics, Menderes Massif, resistivity.

Introduction

The study area is situated near the southern edge of the Menderes Massif in south-western Turkey. The Menderes Massif bears several Fe-rich emery bodies and is also rich in metallic and non-metallic minerals, such as iron, chrome, copper, lead, zinc, mercury, gold, silver, uranium, coal, feldspar, kaolin and bauxite (Smith, 1850; Yalcin et al., 1993; Gümüş et al., 1999; J. Wippern, unpubl. data). Many geoscientists, therefore, have been interested in the Menderes Massif for its special tectonic and geological characteristics and various mineral deposits. Various mining activities have taken place in the Massif since ancient times, and many of these activities have not been reported or published.

Emery rocks are mainly composed of alumina and iron minerals. It occurs naturally in the Aegean region, mostly in Turkey and Greece. Due to its hardness (hardness degree 9), it is used in the manufacturing of resistant surfaces, grinding wheels, vehicle parts and refractory brick, as well as in the optic industry.

The primary objective of this geophysical survey is to provide new data for emery producers and research geoscientists. To meet these objectives, we used our available magnetic and electrical equipment over two field trips of a week each, with a limited project budget, in the study area which was 380 km far away from the university campus in Isparta city. Although there has been research on geology, petrology and mineral chemistry of emery deposits worldwide (Yalcin et al., 1993; Feenstra, 1996, 1997), we could not find any publications or reports relating to the geophysical surveys of emery fields in the available literature. Therefore, the study presented here can be viewed as a general case history on the application of geophysical methods for emery deposits.

Geological setting

Regional geology

The Menderes Massif consists of mainly Paleozoic or Precambrian augen-gneiss, which forms the core of the Massif, Permocarboniferous schists, Santonian-Campanian thick-bedded limestone units and marble hills, and intruding Cretaceous granitic to gneissic plutons (Figure 1). The Massif also has mainly E–W- and NE-trending active graben systems that have developed as a result of an extension regime in western Turkey (Şengör et al., 1984; Collins and Robertson, 1997, 1998, 1999). It is tectonically overlain in the south by the Lycian Nappes which crop out in the western part of the Tauride belt. These are composed largely of allochthonous Mesozoic carbonate rocks capped by slabs of peridotite: in the north and north-west by the nappes belonging to the Izmir–Ankara–Erzincan Suture Zone; in the north-east by the Afyon Zone composed of a shelf-type Paleozoic–Mesozoic sequence; and in the north-west by the Bornova Flysch Zone which mainly consists of widespread Mesozoic sediments which lie between the Izmir–Ankara–Erzincan Suture Zone and the Menderes Massif Metamorphics (Bozkurt and Oberhansli, 2001; Okay, 2001; Özer et al., 2001; Collins and Robertson, 2003).

The basement core rock of the Menders Massif is higher-grade augen-gneiss (e.g. orthogneiss) of Paleozoic or Precambrian origin, but does not crop out in the study area. Towards the

 10.1071/EG09004 0812-3985/11/020159

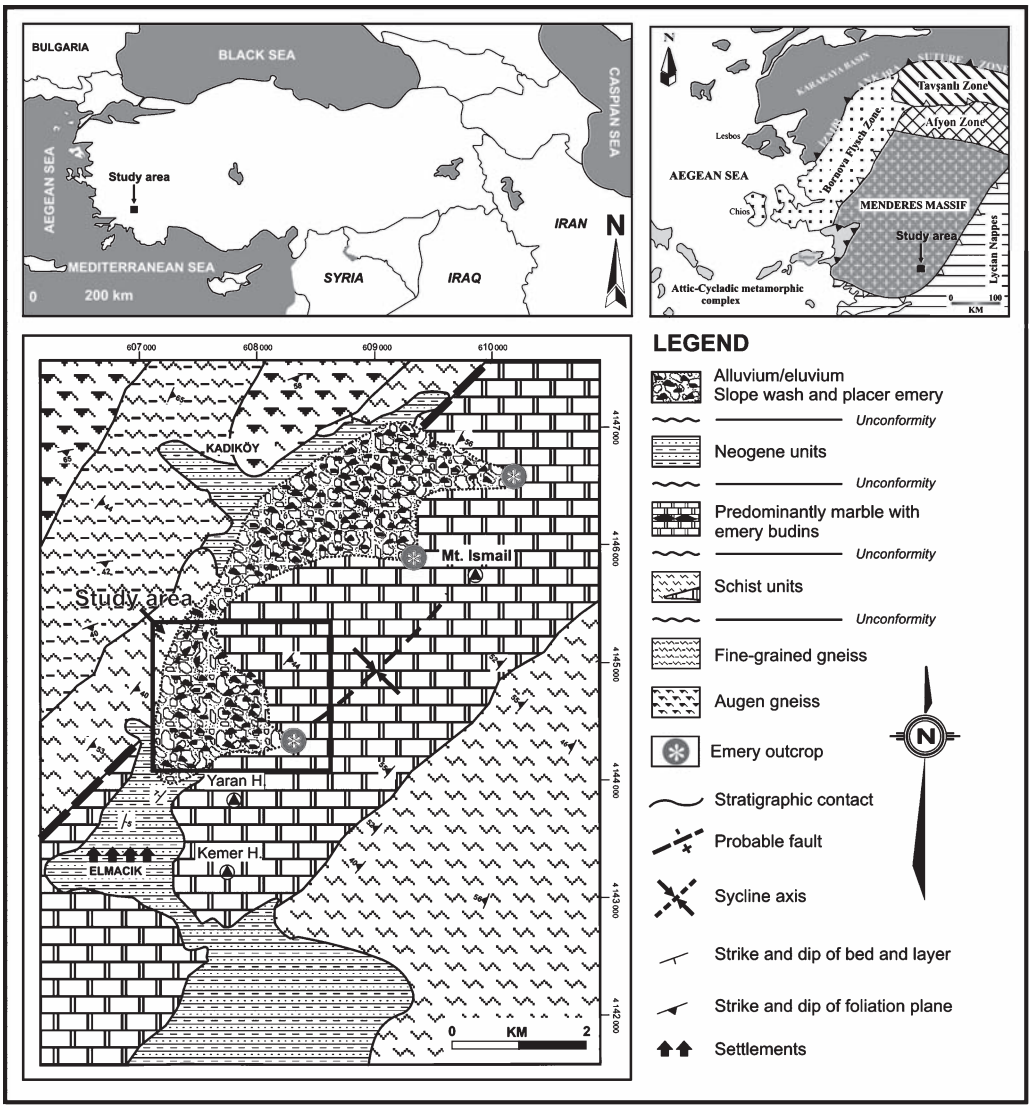

Fig. 1. Regional and local geology of the study area (modified from Aydogan, 2001 and Okay, 2001).

upper levels, the basement rock is a fine-grained Cambrian gneiss (e.g. paragneiss). Permocarboniferous schist intercalated with marble lenses form the lower part of the surface rocks throughout the Menderes Massif, surrounding the basement rocks like an envelope and being overlain by marble units (Okay, 2001).

The Mesozoic metasedimentary rocks, subjected to Alpine metamorphism and mantled by schists along the southern part of the Menderes Massif, contain emery horizons mostly showing boudine structures that developed in the karstic voids of the marbles (Aydogan, 2001). The Neogene conglomerate and claystone units overlie all units disconformably and appear in the south-west of the study area (Figure 1).

Geomorphology and local geology

The study area is bounded by two mountains (Figures 2, 3). To the east, Mt Ismail has an altitude of 1000 m above sea level and trends in a NE–SW direction, and to the south, Mt Yaran has an altitude of 850 m above sea level. The geographical coordinates of the centre of the study area are 28.2210° E and 37.4261° N. The mountains are covered with marble boulders and dense bushes of less than 2 m in height. There are also tall pine trees at the summit of Mt Ismail. The alluvial/eluvial (A/E) part of the area covers 2.5 km^2 at the foothills of these mountains, and supports several kinds of vegetation.

The study area comprises three geological units. Permocarboniferous schist is the oldest rock unit situated in the north-west corner of the area. The thick-bedded marbles from the Upper Cretaceous contain primary type Fe-rich emery horizons, and cover two mountains being the largest part of the study area (Figures 2, 3). The third unit is the A/E part in which placer type emery horizons are expected.

The slopes of the mountains and the two creeks probably cause pebbles and gravels to roll down and accumulate at the surface and subsurface of the A/E part (Figure 3). Four old pit-hollows with horizontal dimensions of ~4 × 4 m and depths of ~2 m are present on the A/E plain. These hollows were dug to inspect and/or dig out emery pebbles instead of expending greater effort digging emery from the hard marble unit.

The primary type emery horizons are deposited in the marble in different ways, such as discontinuous patches, massive bodies, layers, breccias and boudine-like structures in the western flank of Mt Ismail, these having been exploited in the past and being marked with the symbols Pit-1, Pit-2 and Pit-3 on the map (Figure 3). Aydogan (2001) suggests that primary emery deposits are usually less than ~200 m long, and 1 to 5 m thick. The abandoned pits have lengths, widths and depths varying from 5 to 20 m, 3 to 5 m and 2 to 3 m, respectively. According to Aydogan (2001), the emery horizons seen at several locations

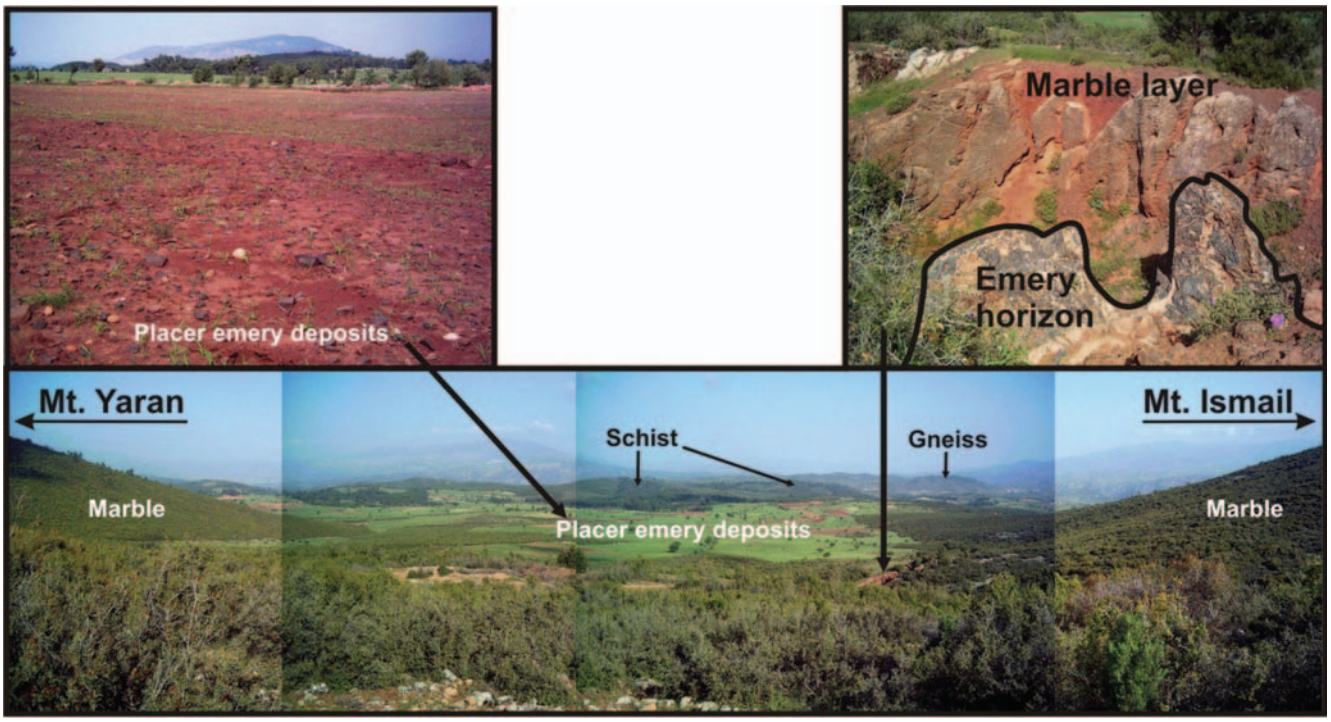

Fig. 2. A panoramic view of the study area from the south-east.

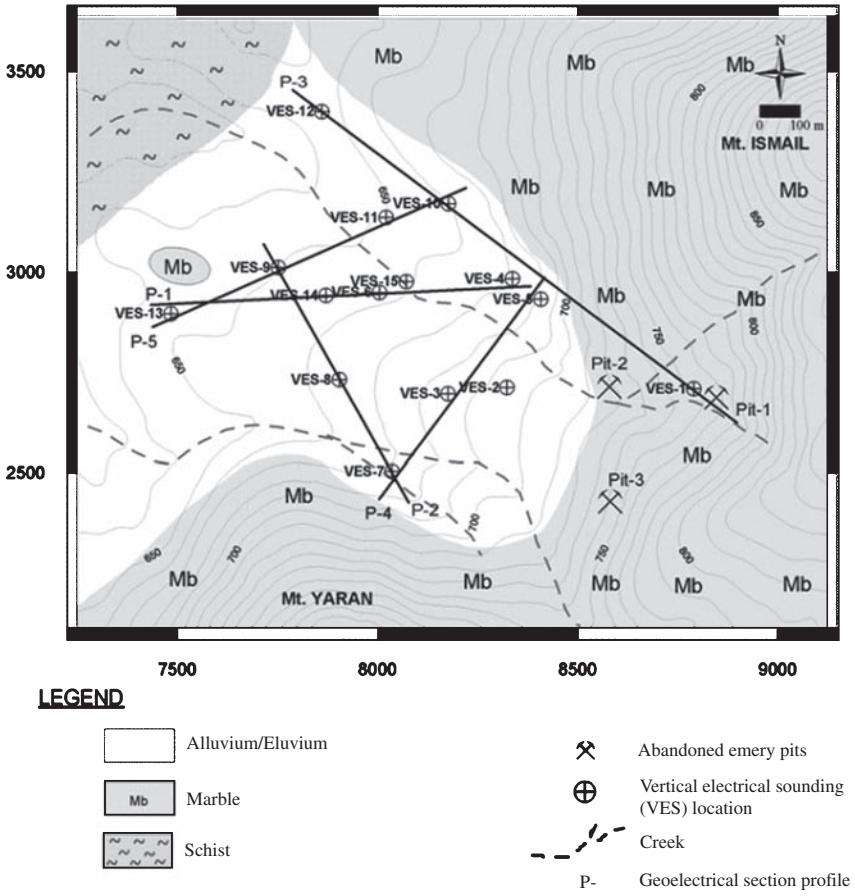

Fig. 3. Local geology and locations of the vertical electrical soundings and cross-section profiles.

on Mt Ismail and Mt Yaran, originated in the karstic-type voids of metacarbonates, and are cut through by aragonite, calcite, chloritoid and margarite veins in the southern part of the study area. They are also formed in the limbs of the isoclines of recumbent folds on Mt Ismail. Evidence such as calcite-filled fissures, folding of the emery horizons, and breccia formations

around the outcrops of Pit-2 and Pit-3 suggest that a probable fault lies along the line connecting these two pits. Emery outcrops in the trenches of Pit-2 and Pit-3 are discontinuous and are the crushed and folded forms. The placer type emery horizons expected in the A/E part might originate from the particles, gravels, pebbles and blocks of these emery horizons and deposits.

Based on the mineralogical and petrographical investigations, coexisting minerals of emery rocks are characterised by a complex mosaic of corundum, diaspore, chloritoid, ilmenite, ilmeno-hematite, rutile, margarite, magnetite and hematite. Corundum is a common mineral in the emery rocks of the Menderes Massif (Figure 4), and contains abundant euhedral ilmenite and titanomagnetite inclusions. The Fe_2O_3 content of five emery samples taken from Pit-1, Pit-2 and Pit-3, and measured by X-ray diffraction analysis, varies between 30.0 and 38.33% (Aydogan, 2001).

Geophysical survey data and interpretation

In order to explore the continuation of the massive emery horizons in the marble unit and placer emery deposits in the subsurface of the A/E part, a geophysical survey using magnetic and electrical methods was carried out in the area. The electrical measurements were concentrated in the A/E part of the study area to search for undulations – if any exist – on the surface of the basement rock, on which emery pebbles might roll and collect. We expected to find magnetic anomalies which were caused by the Fe-rich emery horizons in the marble units and the emery deposits in the depressed areas of the basement rock since the susceptibility of five samples taken from the pits ranged from 400×10^{-6} SI to $71\,500 \times 10^{-6}$ SI.

Total magnetic field intensity measurements were taken at 260 stations with a nominal station interval of 25 m along 14 profiles and randomly distributed stations in the study area and its vicinity (Figure 5). Profile length ranged from 600 to 1600 m, aligned in the E–W direction. Measurements were carried out using a proton magnetometer with an accuracy of 1 nT. Nominal profile spacing was chosen to be 75 m. Taking into account the geological and morphological conditions and gradients of the observed magnetic data, profile spacing was increased to more than 100 m in some places. A magnetometer with a continuous-reading feature would provide an advantage for mapping shorter wavelength anomalies and the modelling of them, but we did not have access to such a system. The coordinates of the stations were determined by means of a Global Positioning System (GPS) with an accuracy of 5 m. Diurnal variations in the geomagnetic field were corrected by repeating the first or last station measurements of the last profile (within 24 h). The Kandilli Observatory (Istanbul) records were also examined to check changes of short duration. Thus, all magnetic data were reduced to a certain hour of a certain day. The magnetic anomaly map shown in Figure 5 was produced from the 25 m × 25 m gridded data after subtracting the mean value of 45 750 nT from the observed data. The maximum and minimum magnetic field intensities vary between about –220 nT at the negative flanks and +180 nT at the positive flanks.

After carrying out the magnetic survey, two types of magnetic anomaly with remarkable characteristics were observed in the study area. The first, short wavelength, anomalies occur in the vicinity of the old abandoned pits and in the A/E part along the Mt Yaran and Mt Ismail foothills. These imply the presence of primary emery horizons around the abandoned pits in the marble unit and placer type horizons in the A/E part. The low intensity and very short wavelength anomalies obtained at some places in the A/E part are probably due to small sized Fe-rich emery deposits.

The most prominent characteristic of anomalies which lie in the marble is that the direction of the magnetic field differs from the present geomagnetic field direction with the inclination angle of 54 degrees and declination angle of 4 degrees (Figure 5). As there have not been any satisfactory studies on this situation, it may be suggested that magnetic reversal, regional and local tectonics and anticlockwise rotation of Western Turkey caused the resultant anomaly pattern individually or, most probably, in combination.

The second type of anomaly which is of lower intensity was found in the middle of the A/E plain and lies predominantly in a NW–SE direction (Figure 5). This widespread anomaly was probably caused by an assembly of successive clay and silty layers which contain Fe-rich emery grains and particles. For the purpose of locating the anomaly generating bodies and outlining their borders, we prepared an analytical signal map from the 25 m × 25 m gridded magnetic data (Figure 6). It is seen in the signal map that the highest amplitudes of the signals occur in the vicinity of the abandoned pits. It should be noted that difference in the profile spacing (nominally 75 m) and station interval (nominally 25 m) probably effected anomaly pattern and anomaly trends, and also caused a shift in anomaly locations.

Before starting the electrical sounding measurements, we made resistivity measurements with 0.5 m to 5 m electrode separations in E–W and N–S directions on the emery outcrops, marbles and schists and on the Neogene unit just outside the study area, in order to get an idea about the intrinsic resistivity values of the units. The resistivity of the marbles varied between 200 and 10 000 Ωm depending on the crystal-size-dependent

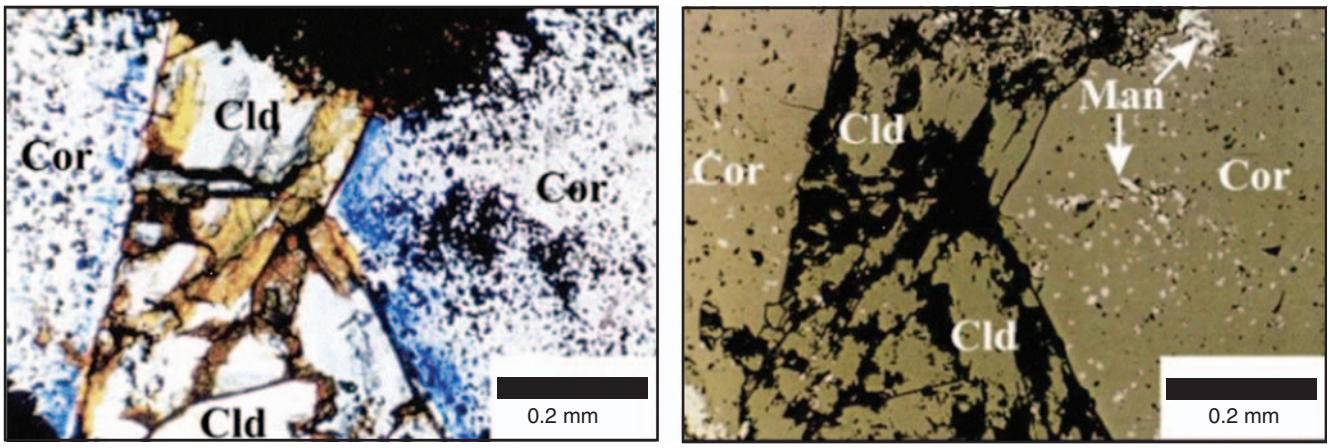

Fig. 4. Photomicrographs of thin- and polished-sections of corundum-rich metabauxites: Cld = chloritoid, Cor = corundum, Man = magnetite.

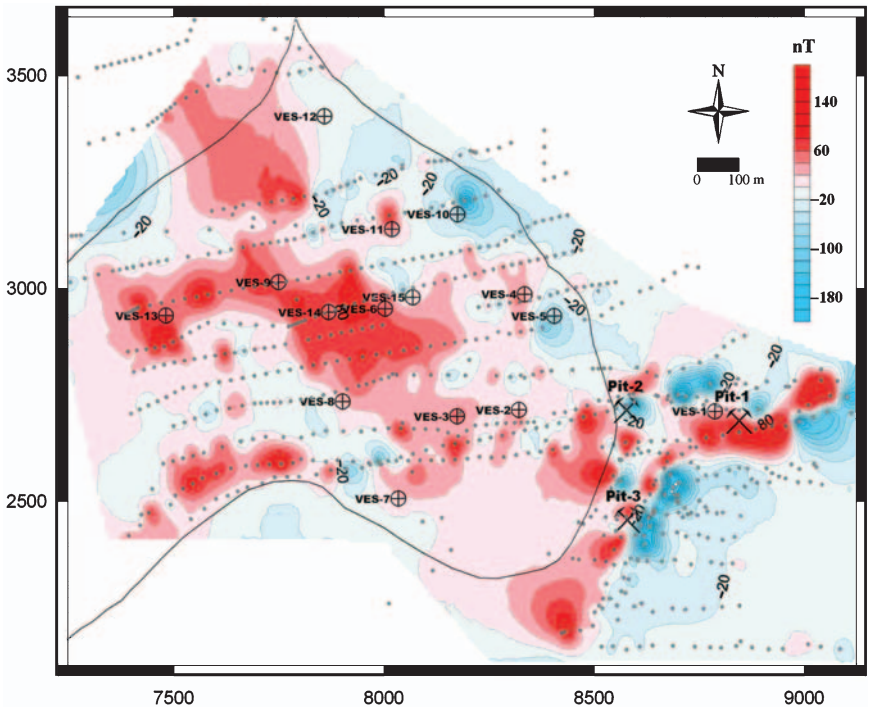

Fig. 5. Magnetic anomaly map. Dots indicate the observation stations. The grey line indicates the alluvial/eluvial plain border.

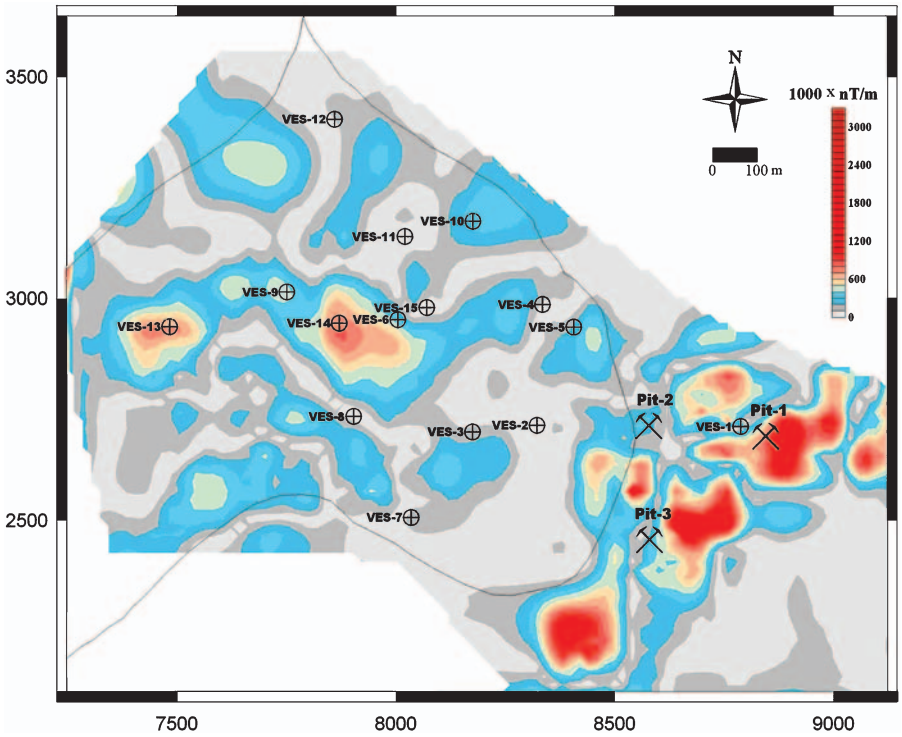

Fig. 6. Analytical signal map of the magnetic data. The grey line indicates the alluvial/eluvial plain border.

texture and fractural structure, and more than 10 000 Ωm where voids were present. Resistivity ranged from 100 to 600 Ωm for the schist and 30 to 80 Ωm for the Neogene units. The upper levels of the schists have been subjected to alteration because of surface or groundwater. The resistivity values obtained over the massive emery outcrops varied from 500 to 4000 Ωm.

Vertical electrical soundings (VES) at the 15 locations on the A/E part were performed with a Schlumberger electrode configuration to investigate the basement depth beneath the A/E part and horizontally bedded emery deposits in the depressed parts of the basement. The VES locations and the direction of electrode spread were selected by considering the predicted direction of movement of the emery material over the slopes and the direction of creek flow.

The density of bushes, marble boulders, and fences and walls around the borders of the wheat, corn, tobacco and melon farms in

the A/E sector of the study area also affected the selection of the VES locations and electrode spread directions. Furthermore, the maximum half-space between current electrodes varied from 100 to 450 m and electrode-spread directions differed at all VES stations depending on these physical conditions. Because of the restrictions all mentioned above, we could not gather electrical data at equally spaced locations. Therefore, we have given priority to constructing the underground resistivity models by using 1D inversion results instead of 2D (Dahlin, 1996; Basokur, 1999). Apparent resistivity curves and their 1D inversion were obtained from IPI2win software developed by Bobachev (2002).

To illustrate the discontinuities and underground structures along the five lines which have been shown with notations P-1 to P-5 in Figure 3, we tried to construct the resistivity cross-sections putting the 1D inversion results on the profiles (Figure 7). In order to form reasonable subsurface geophysical 2D models and 3D geological models which correlate with reasonable geological considerations, we allowed the misfit to rise to around 7% in the 1D models of VES-1, VES-2, and VES-13.

The wide range of resistivity in the layers and lenses assembly of the A/E part of the survey area depends upon two factors. One is the clay and silt content, the other is the presence of Fe-rich emery particles, grains or pebbles at varying rates and sizes. The A/E assembly comprises four successive layers that are intercalated in some levels. The content and resistivity of the lowest to upper levels are interpreted in the following paragraphs.

The lowest succession overlaying the marble unit at the bottom is silty-sandy gravel with resistivity varying between 100 and 300 Ωm. The second succession overlays this and consists of marble sands with clay and silt. Its resistivity is in the range of 50–100 Ωm. The third succession has clay-sand silt closures and resistivities lower than 50 Ωm. The upper-most succession of the assembly is the silty-sandy clay horizon, which has the lowest resistivity ranging between 5 and 40 Ωm.

From cross-sections 3 and 4 and the geological information obtained near local ground water exploration wells, a block diagram was constructed to show locations, depths and thicknesses of the units (Figure 8). This provides a clear spatial picture of the units and tectonic structure in the study area.

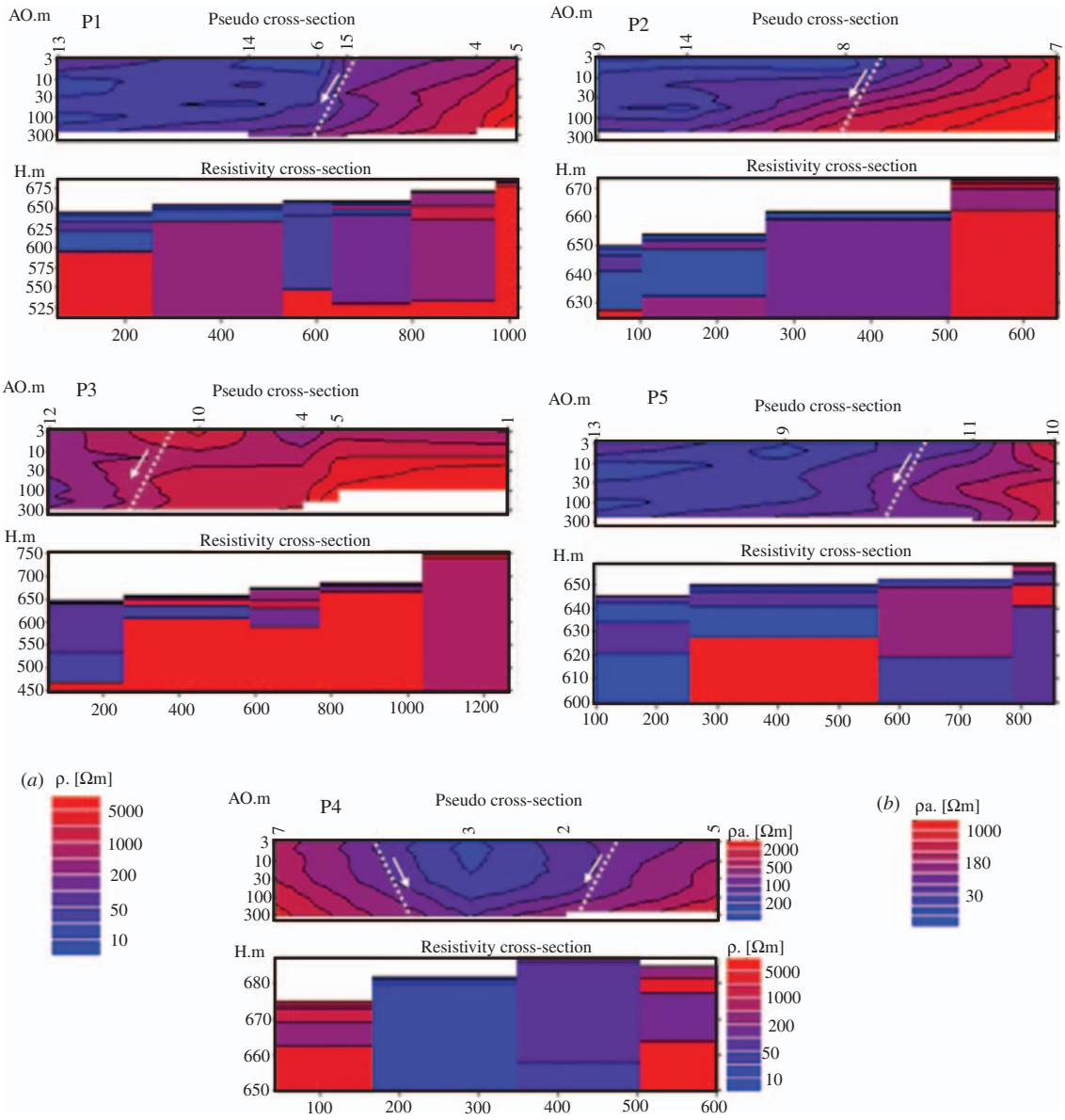

Fig. 7. Cross-sections of the lines from P1 to P5 (see Figure 3). The letters (*a*) and (*b*) indicate the resistivity scale and apparent resistivity scale of lines P1, 2, 3 and 5, respectively. Cross-sections were prepared by using the Bobachev (2002) routine.

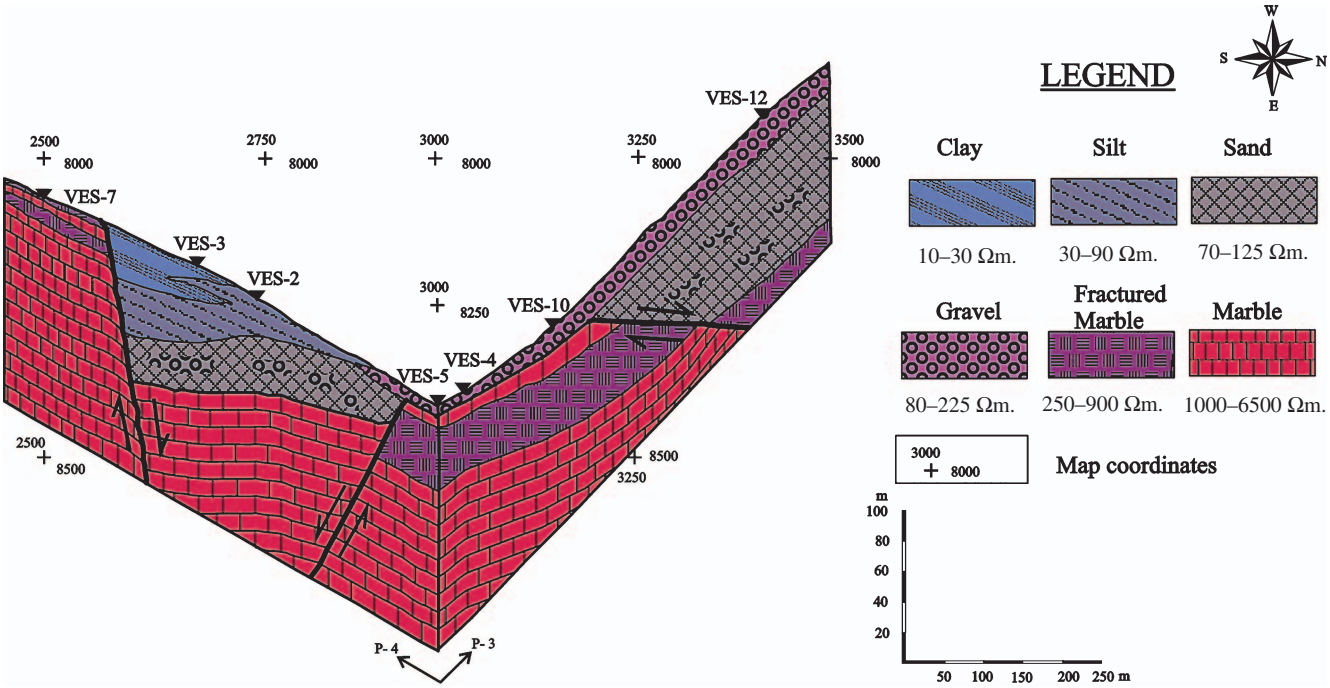

Fig. 8. Block diagram, interpreted from cross-sections of the geoelectrical cross-sections P-3 and P-4 (see Figures 3, 7, 8).

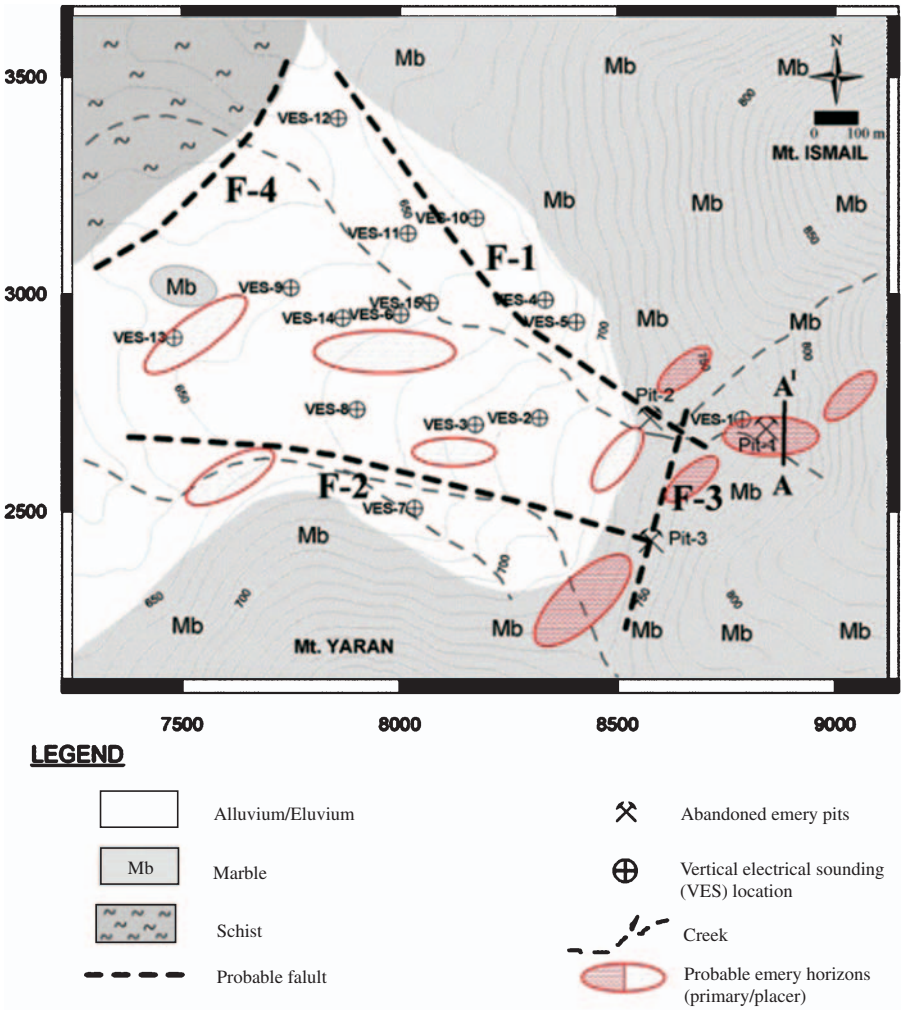

Fig. 9. Interpretation map prepared from the electrical and magnetic data.

First of all, it should be noted that interpretation map in Figure 9 reveals only the individual interpretation of magnetic and electrical data. The marble unit and some sectors of A/E assembly which do not contain emery particles and pebbles do not have significant magnetic features. Resistivities of the massive emery horizons were in the range of the marble units. However, susceptibilities of the emery and marble were significantly different. Additionally, resistivity of the marble is much higher than the average resistivity of the A/E assembly. Therefore, the faults F-1 and F-2, running in an approximate NW–SE direction, were drawn according to the resistivity differences between marble and A/E assembly. The signature of the contour lines seen between Pit-2 and Pit-3 in the magnetic anomaly map was interpreted as a third fault F-3 (Figures 5, 6, 9). The susceptibility difference between marble and magnetite containing emery and geological evidences mentioned above support this suggestion. Although we do not have any geophysical evidence, the fourth fault F-4 might be considered as the continuation of a probable fault between the schist and marble units, as indicated in Figure 1.

Geoelectrical measurements indicated that the A/E assembly consists of several layers with different resistivity values depending upon particle size and clay content, and overlays the marbles of Mt Ismail and Mt Yaran (Figures 7, 8).

Conclusions

In spite of constraints, such as the limited type of geophysical equipment, time, budget and the 380 km distance between campus and the study area, the gathered magnetic and electrical data were interpreted and results were evaluated. Finally we concluded that:

1) The short wavelength and high amplitude magnetic anomalies might be caused by Fe-rich emery bodies located around the old abandoned pits, particularly eastward of Pit-1. The depths to the boudine-like bodies are not more than 10 m in the marble unit.
2) The long wavelength anomaly situated at the centre of the A/E part might originate from a layered horizon bearing Fe-rich emery particles and sands.
3) The successive layers in the A/E assembly showed various resistivity values depending upon their various clay, silt, sand and gravel contents.
4) The A/E assembly has a depth of 70 m in the middle of the study area, and deepens towards the west.
5) Small new emery deposits may be discovered around the old abandoned pits, along the Mt Yaran foothill and in the triangle formed by VES-6, VES-8 and VES-14 (Figure 9). A magnetic survey with denser station intervals should be carried out particularly to the E and NE of Pit-1 and NE and SE of Pit-3.
6) An electromagnetic survey may help for exploring new emery horizons in particularly resistive marble units. Microgravity applications may not give the expected results because of rough topography of the mountainous part of the area.

Acknowledgements

This study was financially supported by a grant from the Research Foundation Office of Suleyman Demirel University (Turkey), project number: 0813-M-04. The authors are deeply indebted to Professor Omer T. Akinci for his encouragement during the project. The authors also thank Mrs Cemile Ozturk and Mr Ali Etiz for their great effort in the acquisition of the geophysical data.

References

Aydogan, M. S., 2001, The research of the emery occurrences at the Elmacik, Mt Ismail (Mugla-Yatagan): Sciences Institute Suleyman Demirel University, M.Sc. Thesis, pp. 53 (in Turkish with English abstract).

Basokur, A. T., 1999, Automated 1D interpretation of resistivity soundings by simultaneous use of the direct and iterative methods: *Geophysical Prospecting*, **47**, 149–177. doi:10.1046/j.1365-2478.1999.00123.x

Bobachev, A. A., 2002, IPI2Win: Moscow State University, Moscow.

Bozkurt, E., and Oberhansli, R., 2001, Menderes Massif (Western Turkey): structural, metamorphic and magmatic evolution – a synthesis: *International Journal of Earth Sciences*, **89**, 679–708. doi:10.1007/s005310000173

Collins, A. S., and Robertson, A. H. F., 1997, The Lycian Melange, south-west Turkey: an Emplaced accretionary complex: *Geology*, **25**, 255–258. doi:10.1130/0091-7613(1997)025<0255:LMSTAE>2.3.CO;2

Collins, A. S., and Robertson, A. H. F., 1998, Processes of Late Cretaceous to Late Miocene episodic thrust-sheet translation in the Lycian Taurides, SW Turkey: *Journal of the Geological Society*, **155**, 759–772. doi:10.1144/gsjgs.155.5.0759

Collins, A. S., and Robertson, A. H. F., 1999, Evoluton of the Lycian allochthon, western Turkey, as a north-facing Late Palaeozoic-Mesozoic rift and passive continental margin: *Geological Journal*, **34**, 107–138. doi:10.1002/(SICI)1099-1034(199901/06)34:1/2<107::AID-GJ817>3.0.CO;2-L

Collins, A., and Robertson, A. H. F., 2003, Kinematic evidence for Late Mesozoic-Miocene emplacement of the Lycian allochton over the Western Anatolide Belt, SW Turkey: *Geological Journal*, **38**, 295–310. doi:10.1002/gj.957

Dahlin, T., 1996, 2D resistivity surveying for environmental and engineering applications: *First Break*, **14**, 275–283.

Feenstra, A., 1996, An EMP and TEM-AEM study of margarite, muscovite and paragonite in polymetamorphic metabauxites of Naxos (Cyclades, Greece) and the implications of fine-scale mica interlayering and multiple mica generations: *Journal of Petrology*, **37**, 201–233. doi:10.1093/petrology/37.2.201

Feenstra, A., 1997, Zincohogbomite and gahnite in a diaspore-bearing metabauxite from eastern Samos (Greece): mineral chemistry, element partitioning and reaction relations: *Schweizerische Mineralogische und Petrographische Mitteilungen*, **77**, 73–93.

Gümüş, A., Kokturk, U., Dayal, A., and Ozer, S., 1999, Formation and economical potential of emery deposits in the south of the Menderes Massif: First Symposium on Raw Material Resources in western Anatolia, 8–14 March 1999, Izmir (in Turkish).

Okay, A. I., 2001, Stratigraphic and metamorphic inversions in the central Menderes Massif: a new structural model, International Journal of Earth Sciences, Special Issue: Menderes Massif (Western Turkey): Structural, metamorphic and magmatic evolution, **4**, 709–727.

Özer, S., Sözbilir, H., Özkar, İ., Toker, V., and Sarı, B., 2001, Stratigraphy of Upper Cretaceous-Paleogene sequences in the southern and eastern Menderes Massif (western Turkey): *International Journal of Earth Sciences*, **89**, 852–866.

Smith, J. L., 1850, Memoir on metabauxite – First part on geology and mineralogy of metabauxites, from observations made in Asia Minor: *American Journal of Science*, **10**, 354–369.

Şengör, A. C. M., Satır, M., and Akkok, R., 1984, Timing of tectonic events in the Menderes Massif, Western Turkey, Implications for tectonic evolution and evidence for Pan-African basement in Turkey: *Tectonics*, **3**, 693–707. doi:10.1029/TC003i007p00693

Yalcin, U., Schreyer, W., and Medenbach, O., 1993, Zn-rich hogbomite formed from gahnite in the metabauxites of the Menderes Massif, SW Turkey: *Contributions to Mineralogy and Petrology*, **113**, 314–324. doi:10.1007/BF00286924

Manuscript received 31 January 2009; accepted 5 February 2011.